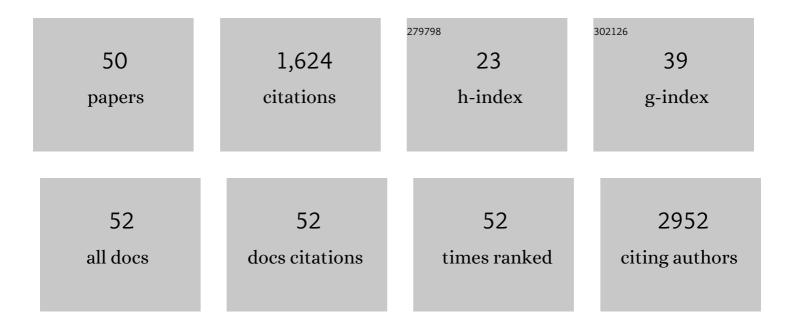
Jessica C Sieren

List of Publications by Year in descending order

Source: https://exaly.com/author-pdf/2926476/publications.pdf Version: 2024-02-01



#	Article	IF	CITATIONS
1	Dynamic regulation of cardiolipin by the lipid pump Atp8b1 determines the severity of lung injury in experimental pneumonia. Nature Medicine, 2010, 16, 1120-1127.	30.7	133
2	COPDGene® 2019: Redefining the Diagnosis of Chronic Obstructive Pulmonary Disease. Chronic Obstructive Pulmonary Diseases (Miami, Fla), 2019, 6, 384-399.	0.7	112
3	Radiomics of Lung Nodules: A Multi-Institutional Study of Robustness and Agreement of Quantitative Imaging Features. Tomography, 2016, 2, 430-437.	1.8	108
4	Alveolar Dynamics during Respiration. American Journal of Respiratory Cell and Molecular Biology, 2008, 38, 572-578.	2.9	98
5	Development and translational imaging of a TP53 porcine tumorigenesis model. Journal of Clinical Investigation, 2014, 124, 4052-4066.	8.2	92
6	Mitochondrial Rac1 GTPase Import and Electron Transfer from Cytochrome c Are Required for Pulmonary Fibrosis. Journal of Biological Chemistry, 2012, 287, 3301-3312.	3.4	78
7	Recent technological and application developments in computed tomography and magnetic resonance imaging for improved pulmonary nodule detection and lung cancer staging. Journal of Magnetic Resonance Imaging, 2010, 32, 1353-1369.	3.4	75
8	Lung structure phenotype variation in inbred mouse strains revealed through in vivo micro-CT imaging. Journal of Applied Physiology, 2010, 109, 1960-1968.	2.5	74
9	Features of COPD as Predictors of LungÂCancer. Chest, 2018, 153, 1326-1335.	0.8	67
10	Sinus hypoplasia precedes sinus infection in a porcine model of cystic fibrosis. Laryngoscope, 2012, 122, 1898-1905.	2.0	61
11	Computed Tomography Measure of Lung at Risk and Lung Function Decline in Chronic Obstructive Pulmonary Disease. American Journal of Respiratory and Critical Care Medicine, 2017, 196, 569-576.	5.6	59
12	Machine learning approach for distinguishing malignant and benign lung nodules utilizing standardized perinodular parenchymal features from CT. Medical Physics, 2019, 46, 3207-3216.	3.0	59
13	Comparison of spirometric thresholds in diagnosing smoking-related airflow obstruction. Thorax, 2014, 69, 410-415.	5.6	53
14	Improved pulmonary nodule classification utilizing quantitative lung parenchyma features. Journal of Medical Imaging, 2015, 2, 041004.	1.5	44
15	A porcine model of neurofibromatosis type 1 that mimics the human disease. JCI Insight, 2018, 3, .	5.0	44
16	Comparison of low―and ultralowâ€dose computed tomography protocols for quantitative lung and airway assessment. Medical Physics, 2017, 44, 4747-4757.	3.0	42
17	Approaches to Evaluate Lung Inflammation in Translational Research. Veterinary Pathology, 2018, 55, 42-52.	1.7	38
18	Longitudinal assessment of lung cancer progression in the mouse using <i>in vivo</i> micro T imaging. Medical Physics, 2010, 37, 4793-4805.	3.0	37

JESSICA C SIEREN

#	Article	IF	CITATIONS
19	RABL6A Is an Essential Driver of MPNSTs that Negatively Regulates the RB1 Pathway and Sensitizes Tumor Cells to CDK4/6 Inhibitors. Clinical Cancer Research, 2020, 26, 2997-3011.	7.0	34
20	An Automated Segmentation Approach for Highlighting the Histological Complexity of Human Lung Cancer. Annals of Biomedical Engineering, 2010, 38, 3581-3591.	2.5	29
21	Understanding the Redox Biology of Selenium in the Search of Targeted Cancer Therapies. Antioxidants, 2020, 9, 420.	5.1	29
22	CT-derived Biomechanical Metrics Improve Agreement Between Spirometry and Emphysema. Academic Radiology, 2016, 23, 1255-1263.	2.5	26
23	Exploration of the volumetric composition of human lung cancer nodules in correlated histopathology and computed tomography. Lung Cancer, 2011, 74, 61-68.	2.0	24
24	Immunohistochemical Markers for Prospective Studies in Neurofibromatosis-1 Porcine Models. Journal of Histochemistry and Cytochemistry, 2017, 65, 607-618.	2.5	21
25	Differentiation of non-small cell lung cancer and histoplasmosis pulmonary nodules: insights from radiomics model performance compared with clinician observers. Translational Lung Cancer Research, 2019, 8, 979-988.	2.8	20
26	A CT-Based Automated Algorithm for Airway Segmentation Using Freeze-and-Grow Propagation and Deep Learning. IEEE Transactions on Medical Imaging, 2021, 40, 405-418.	8.9	17
27	Impact of advanced detector technology and iterative reconstruction on lowâ€dose quantitative assessment of lung computed tomography density in a biological lung model. Medical Physics, 2018, 45, 3657-3670.	3.0	15
28	Longitudinal phenotype development in a minipig model of neurofibromatosis type 1. Scientific Reports, 2020, 10, 5046.	3.3	13
29	Expert consensus on perioperative immunotherapy for local advanced non-small cell lung cancer. Translational Lung Cancer Research, 2021, 10, 3713-3736.	2.8	12
30	Disproportionate Contribution of Right Middle Lobe to Emphysema and Gas Trapping on Computed Tomography. PLoS ONE, 2014, 9, e102807.	2.5	12
31	Assessment of nociception and related quality-of-life measures in a porcine model of neurofibromatosis type 1. Pain, 2019, 160, 2473-2486.	4.2	11
32	CT-Assessed Dysanapsis and Airflow Obstruction in Early and Mid Adulthood. Chest, 2022, 161, 389-391.	0.8	10
33	Radiomic biomarkers informative of cancerous transformation in neurofibromatosis-1 plexiform tumors. Journal of Neuroradiology, 2019, 46, 179-185.	1.1	9
34	A Risk Prediction Model for Mortality Among Smokers in the COPDGene® Study. Chronic Obstructive Pulmonary Diseases (Miami, Fla), 2020, 7, 346-361.	0.7	9
35	A Process Model for Direct Correlation between Computed Tomography and Histopathology. Academic Radiology, 2010, 17, 169-180.	2.5	7
36	Factors Affecting Radiation Dose in Computed Tomography Angiograms for Pulmonary Embolism: A Retrospective Cohort Study. Journal of Clinical Imaging Science, 2020, 10, 74.	1.1	7

JESSICA C SIEREN

#	Article	IF	CITATIONS
37	Computed Tomography and Magnetic Resonance Imaging for Longitudinal Characterization of Lung Structure Changes in a Yucatan Miniature Pig Silicosis Model. Toxicologic Pathology, 2016, 44, 373-381.	1.8	6
38	Information theory optimization based feature selection in breast mammography lesion classification. , 2018, , .		6
39	Post-imaging pulmonary nodule mathematical prediction models: are they clinically relevant?. European Radiology, 2019, 29, 5367-5377.	4.5	6
40	Protein Kinase Cζ Inhibitor Promotes Resolution of Bleomycin-Induced Acute Lung Injury. American Journal of Respiratory Cell and Molecular Biology, 2016, 55, 869-877.	2.9	5
41	Comparison of spirometric thresholds in diagnosing smoking-related airflow obstruction: authors' response. Thorax, 2014, 69, 1147-1148.	5.6	4
42	High-energy external defibrillation and transcutaneous pacing during MRI: feasibility and safety. Journal of Cardiovascular Magnetic Resonance, 2019, 21, 47.	3.3	4
43	Porcine cancer models for translational oncology. Molecular and Cellular Oncology, 2014, 1, e969626.	0.7	3
44	Quantitative Imaging Markers of Lung Function in a Smoking Population Distinguish COPD Subgroups with Differential Lung Cancer Risk. Cancer Epidemiology Biomarkers and Prevention, 2019, 28, 724-730.	2.5	3
45	Menstrual cycle impacts lung structure measures derived from quantitative computed tomography. European Radiology, 2021, , 1.	4.5	3
46	Validating indicators of CNS disorders in a swine model of neurological disease. PLoS ONE, 2020, 15, e0228222.	2.5	2
47	Computed Tomography Features of Lung Structure Have Utility for Differentiating Malignant and Benign Pulmonary Nodules. Chronic Obstructive Pulmonary Diseases (Miami, Fla), 2022, 9, 154-164.	0.7	1
48	Scanner-specific validation of a CT simulator using a COPD-emulated anthropomorphic phantom. , 2022, 12031, .		1
49	Consistent and reproducible positioning in longitudinal imaging for phenotyping genetically modified swine. , 2015, , .		Ο
50	Inter- and intra-scan variability for lung imaging quantifications via CT. , 2022, 12031, .		0